Insulin ameliorates pulmonary edema through the upregulation of epithelial sodium channel via the PI3K/SGK1 pathway in mice with lipopolysaccharide-induced lung injury

WANG DENG, CHANG-YI LI, JIN TONG, JING HE, YAN ZHAO and DAO-XIN WANG

Department of Respiratory Medicine, Second Affiliated Hospital of
Chongqing Medical University, Chongqing 400010, P.R. China

Abstract. Epithelial sodium channel (ENaC) provides the driving force for the removal of edema from the alveolar spaces in acute lung injury (ALI). Our previous study reported that insulin increased the expression of α-ENaC, possibly via the serum/glucocorticoid-inducible kinase-1 (SGK1) pathway in ALI; however, the upstream regulator of SGK1 activity remains unclear. In the current study, C3H/HeN mice were subjected to lipopolysaccharide (LPS)-induced lung injury without hyperglycemia. Exogenous insulin was administered intravenously using a micro-osmotic pump, and intratracheal delivery of SGK1 small interfering RNA (siRNA) was performed. Furthermore, alveolar epithelial type II cells transfected with phosphatidylinositol 3-kinase (PI3K) siRNA or SGK1 siRNA were incubated with insulin. Insulin protected the pulmonary epithelial barrier, reduced the apoptosis of alveolar epithelial cells, attenuated pulmonary edema, improved alveolar fluid clearance, and increased the expression levels of α-, β- and γ-ENaC in mice. In addition, in alveolar epithelial cells, insulin increased the expression levels of α-, β- and γ-ENaC, as well as the level of phosphorylated SGK1, which were then inhibited by the selective targeting of PI3K or SGK1 by siRNA. Taken together, the results of the present study demonstrated that insulin protected the lung epithelium and attenuated pulmonary edema through the upregulation of ENaC via the PI3K/SGK1 pathway in LPS-induced lung injury.

Introduction

Acute lung injury (ALI) or acute respiratory distress syndrome (ARDS) refer to a life-threatening clinical syndrome that is characterized by severe hypoxemia and acute respiratory failure, caused by alveolar epithelial injury and accumulation of protein-rich fluid in the alveolar spaces, with in-hospital mortality of 40% (1,2). Improving the outcome of ALI/ARDS requires the clearance of excessive edema in the alveolar spaces and repair of the alveolar epithelium (3).

The epithelial sodium channel (ENaC), which mainly determines the alveolar fluid volume *in vivo*, provides the driving force for the removal of edema from the alveolar spaces, (4-6). ENaC is expressed in the apical membrane of alveolar epithelial type II cells and has been shown to participate in amiloride-sensitive sodium influx. ENaC comprises three homologous subunits, namely α-, β- and γ-ENaC, which share a structure consisting of two hydrophobic membrane-spanning regions, intracellular amino and carboxy termini, two transmembrane spanning domains and a large extracellular loop with highly conserved cysteine residues (7). Previous studies have reported that alveolar edema could not be cleared in mice lacking the α-, β- or γ-ENaC genes, which proves the important role of ENaC in alveolar fluid clearance (AFC) (8-10).

Phosphatidylinositol 3-kinase (PI3K), which contains a catalytic and a regulatory domain, participates in cell survival, migration, metabolism, cytoskeletal rearrangement and vesicular trafficking (11). The PI3K signaling pathway was demonstrated to be integral for the regulation of ENaC by insulin stimulation in kidney cells (12-14). The serum/glucocorticoid-inducible kinase-1 (SGK1), a critical regulatory protein of ENaC, is activated by insulin through the PI3K signaling pathway (15,16). Insulin is considered to dominate the anti-inflammatory function during ALI (17); however, its effect on AFC remains unclear. Our previous study revealed

Correspondence to: Dr Dao-Xin Wang, Department of Respiratory Medicine, Second Affiliated Hospital of Chongqing Medical University, 76 Linjiang Road, Yuzhong, Chongqing 400010, P.R. China
E-mail: 359403841@qq.com

Abbreviations: ENaC, epithelial sodium channel; ALI, acute lung injury; ARDS, acute respiratory distress syndrome; AFC, alveolar fluid clearance; LPS, lipopolysaccharide; PCR, polymerase chain reaction; PI3K, phosphatidylinositol 3-kinase; SGK1, serum/glucocorticoid-inducible kinase-1; TUNEL, terminal deoxynucleotidyl transferase dUTP nick end labeling; BALF, bronchoalveolar lavage fluid; TLR4, Toll-like receptor 4

that insulin upregulated α-ENaC, possibly via the activation of SGK1, in the lung (18). However, whether the PI3K/SGK1 signaling pathway participated in the regulation of ENaC-mediated AFC in ALI has yet to be elucidated.

In the present study, the aim was to investigate the effect of insulin on ENaC expression and the involvement of the PI3K/SGK1 pathway in lipopolysaccharide (LPS)-induced lung injury.

Materials and methods

Animals and materials. A total of 24 C3H/HeN mice (Charles River Laboratories, Inc., Wilmington, MA, USA) aged 7-9 weeks were housed under specific pathogen-free conditions in a temperature- and humidity-controlled environment (temperature: 22±1°C and humidity: 70±10%) with a 12-h light/dark cycle, and given free access to food and water. PI3K p85α small interfering RNA (siRNA) and a scramble non-targeting siRNA (serving as the control) were purchased from Santa Cruz Biotechnology, Inc. (Dallas, TX, USA). SGK1 siRNA was designed and synthesized by Shanghai Gene Pharma Co., Ltd. (Shanghai, China). All animal experiments were conducted in accordance with the Guide for the Care and Use of Laboratory Animals, and approved by the Ethics Committee of the Second Affiliated Hospital of Chongqing Medical University (Chongqing, China).

Animal model and intervention. Mice were anesthetized by intraperitoneal administration of sodium pentobarbital (Sigma-Aldrich; Merck KGaA, Darmstadt, Germany) at a dose of 50 mg/kg. The ALI model was established using LPS (*Escherichia coli* serotype O111:B4; Sigma-Aldrich; Merck KGaA) at a dose of 5 mg/kg in 50 μl sterile phosphate-buffered saline by a one-time intratracheal injection (19). Human insulin (Eli Lilly & Co., Indianapolis, IN, USA) was administered at a dose of 0.1 U/kg/h at a rate of 2.5 mU/h/mouse via an internal jugular vein catheter attached to micro-osmotic pumps at 16 h prior to exposure to LPS. Mice were randomly divided into four groups: i) Control group (n=6); ii) LPS group (n=6); iii) LPS + insulin group (n=6); and, iv) LPS + insulin + SGK1 siRNA group (n=6). Mice in the control group received an equivalent volume of saline. Blood samples were collected from the catheter by centrifugation at 1,500 x g at 4°C for 15 min. Glucose levels in the plasma were recorded at different time points by a glucometer (Johnson & Johnson Medical Ltd., Shanghai, China). Mice were sacrificed by exsanguination from the carotid artery 24 h after LPS administration. Next, bronchoalveolar lavage fluid (BALF) and lung tissue were obtained for analysis.

Primary cell isolation and culture. Alveolar epithelial type II cells were isolated from healthy untreated male C3H/HeN mice, as previously described (20). The cells were cultured in Dulbecco's modified Eagle's medium containing 10% fetal bovine serum, 100 U/ml penicillin and 0.1 mg/ml streptomycin in an atmosphere with 5% CO_2 and 95% air.

siRNA transfection. Alveolar epithelial cells isolated from healthy untreated male C3H/HeN mice were transfected with PI3K siRNA or SGK1siRNA using Lipofectamine®

Table I. Effect of exogenous insulin (0.1 U/kg) on plasma glucose levels in normal mice.

Time after insulin administration (min)	Plasma glucose (mmol/l)
0	4.8±0.5
30	4.9±0.4
60	5.1±0.6
120	5.1±0.5
240	5.3±0.6

Data are presented as the mean ± standard error (n=5 per group).

Table II. Effect of exogenous insulin on plasma glucose levels in mice with LPS-induced lung injury.

	Plasma glucose level (mmol/l)	
Time (h)	LPS	LPS + insulin
0	7.6±0.7	7.1±0.8
1	6.8±0.7	6.5±0.5
4	6.3±0.4	6.2±0.3
8	5.9±0.5	5.7±0.6

Data are presented as the mean ± standard error (n=10 per group).

2000 (Invitrogen; Thermo Fisher Scientific, Inc., Waltham, MA, USA), according to the manufacturer's protocol. At 72 h after transfection, cells were incubated with or without 200 mU/l insulin for 2 h . They were divided into 4 groups: Control group, insulin group, insulin+PI3K siRNA group and insulin+SGK1 siRNA group. Then the alveolar epithelial cells were processed for western blotting. In the mice experiments, intratracheal delivery of siRNA was performed in the mice, as previously described (21). Mice were anesthetized and their tongues were gently pulled out. Then 75 μg siRNA specific for SGK1 was pipetted in vehicle, 100 μl saline, directly into the throat, momentarily blocking the mouse's airway 2 h after LPS exposure in the mice treated with LPS + insulin. An equivalent dose of non-targeting siRNA served as the control in the other mice groups. Inspiration carried the siRNA and vehicle into the lung.

BALF analysis. Normal saline (5 ml) was instilled into the right lung three times. The lavage fluid from the right lung was carefully pooled and centrifuged at 1,700 x g for 30 min at 4°C. The total cell count was then determined by a hemocytometer, and differential cell counts were assessed on cytocentrifuge preparations stained with Diff-Quik (Sigma-Aldrich; Merck KGaA). Total protein in the BALF was determined using a KeyGen assay kit (Nanjing KeyGen Biotech Co., Ltd., Nanjing, China).

Bronchoalveolar epithelial permeability analysis. At 24 h after LPS-induced lung injury, mice were injected with fluorescein isothiocyanate-conjugated dextran 4000 (FD4;
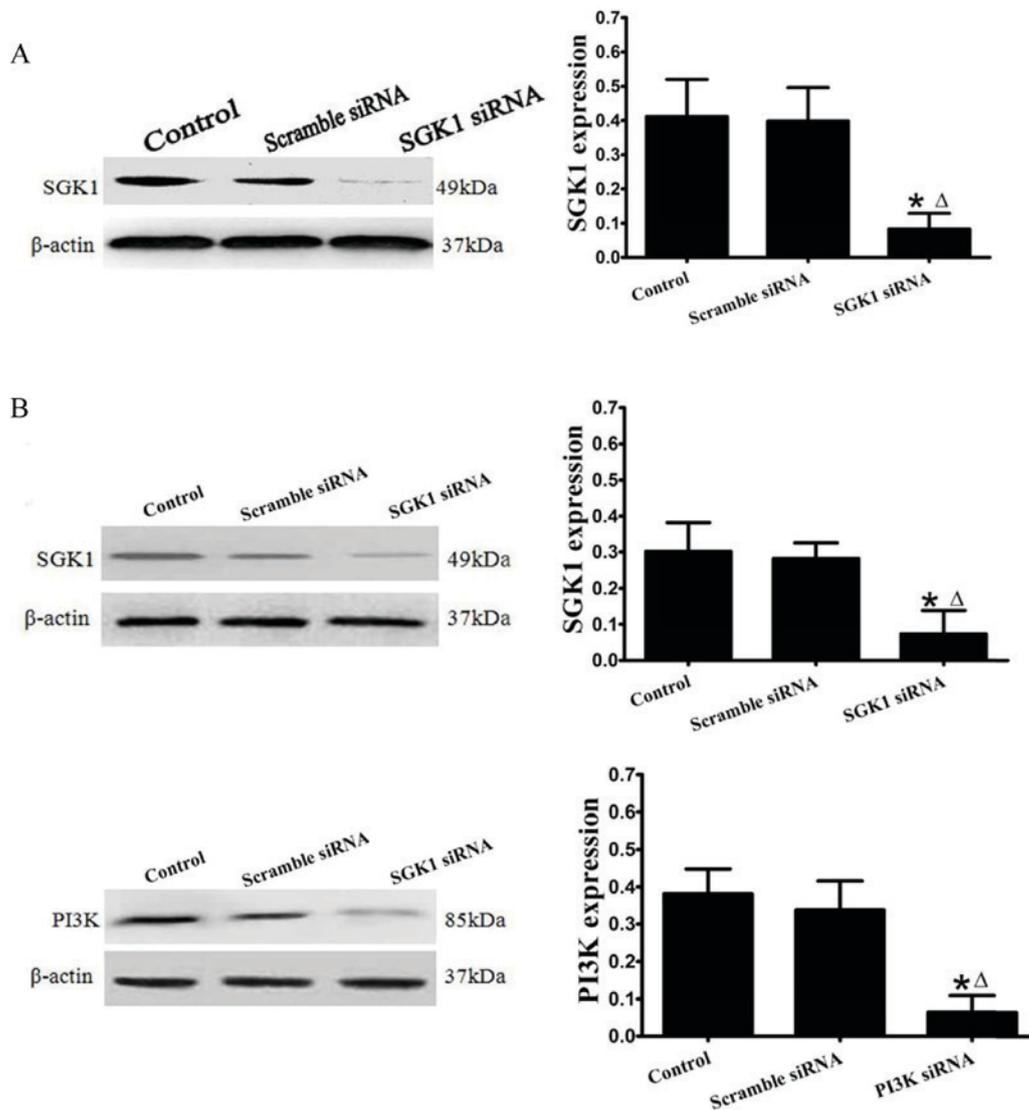
Figure 1. The effect of siRNA transfection in mouse lung tissues and primary alveolar epithelial cells. (A) Western blotting of SGK1 expression in mouse lung tissues following transfection with scramble or SGK1 siRNAs. (B) Primary alveolar epithelial cells were transfected with scramble, PI3K or SGK1 siRNAs, and then subjected to western blotting. Data are presented as the mean ± standard error of the mean. $^{\Delta}$P<0.05 vs. Control; *P<0.05 vs. Scramble siRNA. PI3K, phosphatidylinositol 3-kinase; SGK1, serum/glucocorticoid-inducible kinase-1; siRNA, small interfering RNA.

Sigma-Aldrich; Merck KGaA) solution in PBS (10 mg/kg) via the internal jugular vein. Normal saline (1 ml) was instilled into the lungs three times after 50 min. Subsequently, BALF was carefully collected, and serum was collected from the internal jugular vein blood by centrifugation at 1,500 x g for 5 min. The concentrations of FD4 in the BALF and serum were determined by a spectrofluorometer (BD Biosciences, Franklin Lakes, NJ, USA) using an excitation wavelength of 492 nm and an emission wavelength of 515 nm. Bronchoalveolar epithelial permeability was determined based on the BALF/serum fluorescence ratio.

Hematoxylin and eosin staining. The unlavaged left lungs were harvested 24 h after LPS administration and fixed with 10% neutral buffered formalin for 24 h. The fixed tissues were embedded in paraffin and cut into 5-μm section. Next, the sections were mounted onto glass slides and then stained with hematoxylin for 10 min and eosin for 2 min. Then, 5 random areas were examined at a magnification of x100 for each section. Lung injury was evaluated according to a new histologic lung injury scoring system (22).

Wet-to-dry ratio. The left lungs were isolated to determine the wet-to-dry ratio of the tissue. After the wet weight of the lungs was measured, the lungs were placed in an oven at 80˚C for 48 h and then weighed again in order to obtain their dry weight. Pulmonary edema was determined based on the wet-to-dry ratio; a high ratio indicated more pulmonary edema while low ratio indicated less pulmonary edema compared with normal lungs.

AFC analysis. AFC was measured as previously described (23). Briefly, the isolated right lungs were placed in a humidified incubator at 37˚C and ventilated with 100% nitrogen to remove
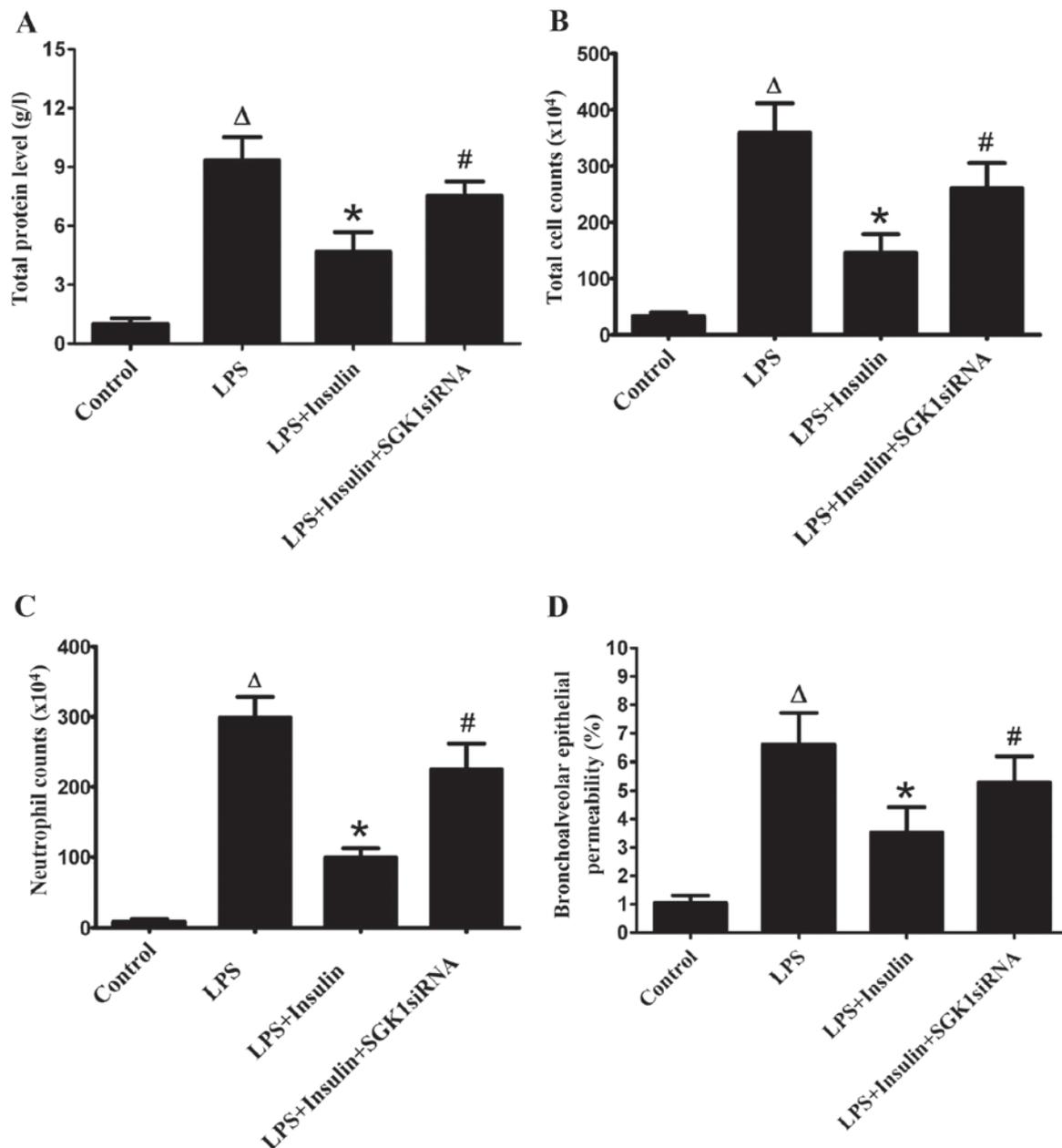
Figure 2. Effect of exogenous insulin on (A) total protein, (B) total cell count and (C) neutrophil count in the bronchoalveolar lavage fluid, and (D) effect on bronchoalveolar epithelial permeability at 24 h after LPS-induced lung injury in mice (n=6 per group). Data are presented as the mean ± standard error. $^{\Delta}$P<0.01 vs. control group; *P<0.01 vs. LPS group; $^{#}$P<0.01 vs. LPS + insulin group. LPS, lipopolysaccharide; SGK1, serum/glucocorticoid-inducible kinase-1; siRNA, small interfering RNA.

oxygen from the alveolar spaces. Physiological saline solution (5 ml/kg) containing 5% albumin and 0.15 mg/ml Evans blue dye (Sigma-Aldrich; Merck KGaA) was injected into the alveolar spaces at an airway pressure of 7 cm H_2O. Alveolar fluid was aspirated 1 h after instillation, and the concentrations of Evans blue-labeled albumin in the injected and aspirated solutions were measured using a spectrophotometer (BD Bioscience). AFC was calculated as follows:

$$AFC = [(Vi\text{-}Vf)/Vi]x100\%$$
$$Vf = (Vi \ x \ Pi)/Pf$$

Vi and Vf represent the injected and final alveolar fluid volume, respectively. Pi and Pf represent the injected and

final concentrations of Evans blue-labeled 5% albumin solution, respectively. Albumin solution containing amiloride (5x10^{-4} M; Sigma-Aldrich; Merck KGaA) was injected into the alveolar spaces.

Terminal deoxynucleotidyl transferase dUTP nick end labeling (TUNEL) assay. Detection of apoptotic cells in the lung epithelium was performed on paraffin-embedded 5-μm lung sections using an *in situ* cell death detection kit (Roche Diagnostics, Indianapolis, IN, USA) by TUNEL reaction. The extent of apoptosis was evaluated by counting the TUNEL-positive cells (brown-stained). TUNEL positive cells were counted in five randomly selected fields (magnification, x400) for each section.
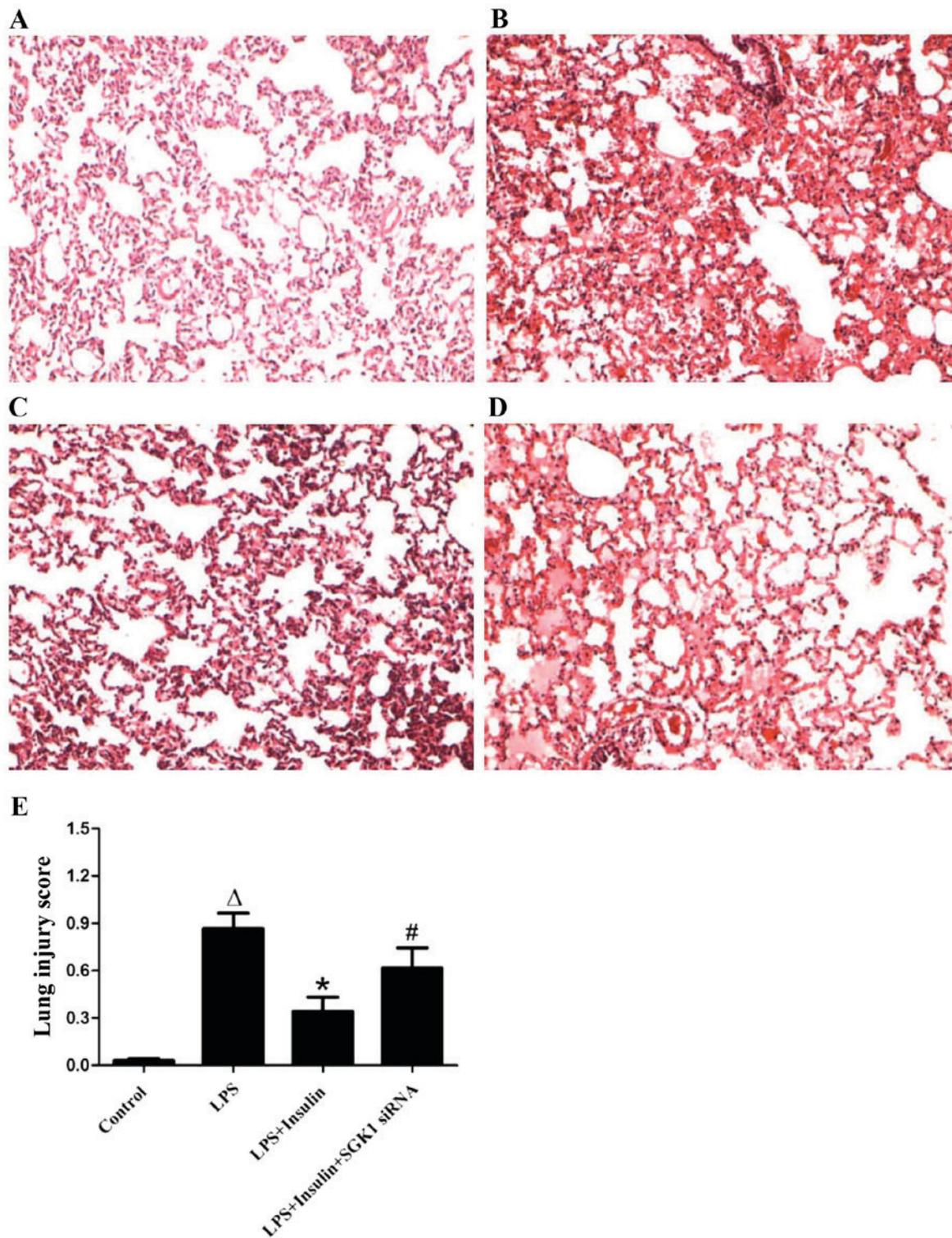
Figure 3. Effect of exogenous insulin on the pulmonary morphology at 24 h after LPS-induced lung injury in mice. (A) Control group, indicating normal pulmonary morphology. (B) LPS group, demonstrating severe interstitial edema, thickened alveolar septa, inflammatory cells and red blood cell infiltration in the alveolar spaces with proteinaceous debris filling the airspaces. (C) LPS + insulin group, demonstrating evident alleviation of interstitial edema, inflammatory cells and red blood cell infiltration in the alveolar space, and of thickened alveolar septa. (D) LPS + insulin + SGK1 siRNA group, demonstrating interstitial edema, inflammatory cells and red blood cell infiltration in the alveolar space, and aggravation of proteinaceous debris. (E) Lung injury score, indicating that insulin significantly attenuated LPS-induced lung injury, while SGK1 siRNA significantly blocked the effect of insulin (n=6 per group). Original magnification, x100. Data are presented as the mean ± standard error. $^{\Delta}$P<0.01 vs. control group; *P<0.01 vs. LPS group; $^{#}$P<0.01 vs. LPS + insulin group. LPS, lipopolysaccharide; SGK1, serum/glucocorticoid-inducible kinase-1; siRNA, small interfering RNA.

Reverse transcription-polymerase chain reaction (RT-PCR). Total RNA was extracted from alveolar epithelial cells following the manufacturer's protocol (Takara Bio, Inc., Otsu, Japan). The concentration and purity of the RNA were estimated using a spectrophotometer. (DU730; Beckman Coulter, Inc., Brea, CA, USA). RT and PCR amplification were performed using an
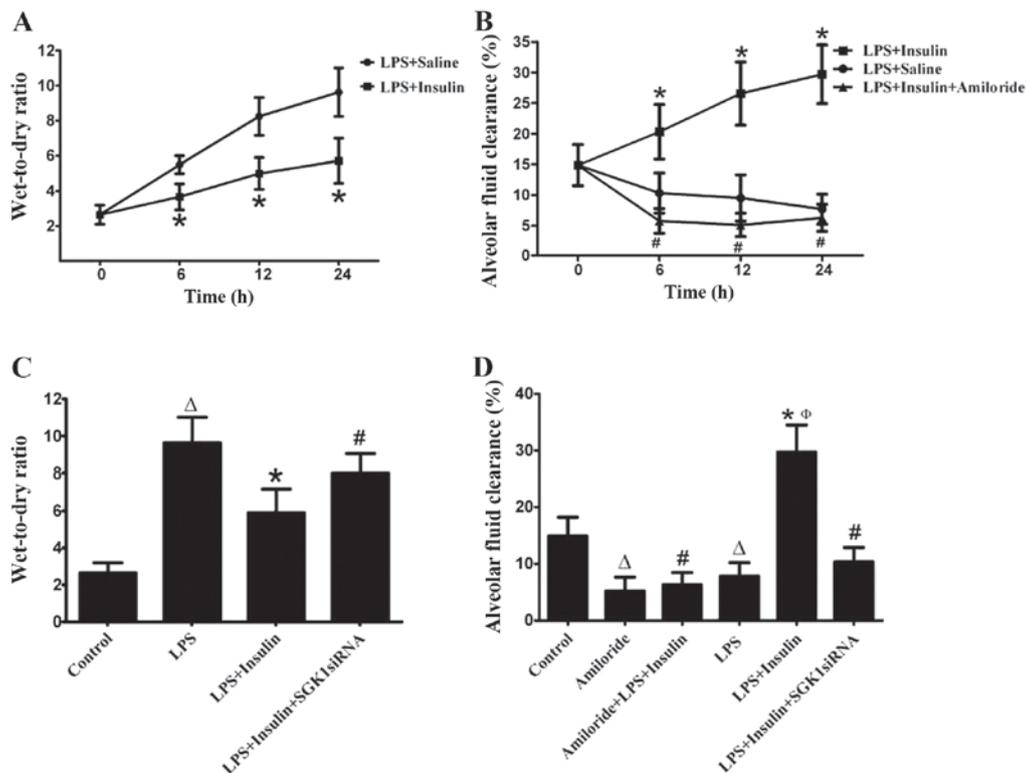
Figure 4. Effect of exogenous insulin on pulmonary edema and alveolar fluid clearance in mice with LPS-induced lung injury (n=6 per group). (A) Wet-to-dry ratio and (B) alveolar fluid clearance at 0, 6, 12 and 24 h in the LPS-induced lung injury group. (C) Wet-to-dry ratio and (D) alveolar fluid clearance at 24 h in the LPS-induced lung injury group. Albumin solution containing amiloride ($5x10^{-4}$ M) was injected into the alveolar spaces 6 h after LPS administration. Data are presented as the mean ± standard error of the mean. $^{\Delta}$P<0.05 vs. control group; $^{\Phi}$P<0.01 vs. amiloride group; *P<0.05 vs. LPS (+ saline) group; $^{#}$P<0.01 vs. LPS + insulin group. LPS, lipopolysaccharide; SGK1, serum/glucocorticoid-inducible kinase-1; siRNA, small interfering RNA.

RT-PCR kit (Takara Bio, Inc.). The RT reaction was conducted at 65˚C for 5 min, 42˚C for 30 min, 95˚C for 5 min and 4˚C for 5 min. The PCR amplification reaction was conducted at 94˚C for 60 sec, followed by 30 cycles at 94˚C for 30 sec, then 53˚C (α-ENaC), 53˚C (β-ENaC), 55˚C (γ-ENaC) or 55˚C (β-actin) for 30 sec, and finally 72˚C for 60 sec. The primer sequences used were: α-ENaC (509 bp), 5'-TACCCTTCCAAGTATACA CAGC-3' (forward) and 5'-CAGAAGGAGACTCCGAATTAG T-3' (reverse); β-ENaC (406 bp), 5'-GCTAAAGAGCTAGCA GTAATGG-3' (forward) and 5'-CTGGTGTTTGTTATGCCT AGAG-3' (reverse); γ-ENaC (363 bp), 5'-GGATCCTGAGAG AGAATCATGC-3' (forward) and 5'-GTGTCCAGCTATGCC CTTTAAC-3' (reverse); β-actin (871 bp), 5'-GTACAACCT TCTTGCAGCTCCT-3' (forward) and 5'-ACAGGATTCCAT ACCCAGGAAG-3' (reverse). PCR products were electrophoresed on 1.0% agarose gels containing ethidium bromide, and images of the gels were captured using a gel imaging system (Bio-Rad Laboratories, Inc., Hercules, CA, USA). The expressions of α-, β- and γ-ENaC were quantified by normalizing the band intensity to β-actin using Quantity One software (version 4.4, Bio-Rad Laboratories, Inc.).

Immunofluorescence assay. Lungs were fixed by immersion in 10% neutral-buffered formalin and embedded in paraffin. The slides with lung sections (5 μm) were soaked in xylene and rehydrated in 100, 95, 85 and 70% solutions of ethanol for 5 min. Following blocking with 10% fetal calf serum for 1 h at room temperature, the sections were incubated with

rabbit polyclonal primary antibodies against α-, β- or γ-ENaC (1:200; sc-21012, sc-21013 and sc-21014 respectively; Santa Cruz Biotechnology, Inc.) overnight at 4˚C. The tissues were then incubated with a goat anti-rabbit secondary antibody labeled with Alexa Fluor 594 (1:400; A-11012; Thermo Fisher Scientific, Inc.) at 37˚C for 1 h. Subsequently, nuclei were stained with DAPI (1:2,000; Sigma-Aldrich; Merck KGaA). Images were captured by confocal laser scanning microscopy (Bio-Rad Laboratories, Inc.) and analyzed using Image-Pro Plus software, version 6.0 (Media Cybernetics, Inc., Rockville, MD, USA).

Western blotting. Total proteins were obtained by incubation with 1 ml lysis buffer and 1 ml extraction buffer using the KeyGen protein extraction kit (Nanjing KeyGen Biotech Co., Ltd., Nanjing, China). The concentration of each protein sample was determined using a BCA protein assay kit (KeyGen Biotech Co., Ltd.). Proteins were then separated by 10% SDS-PAGE and transferred to polyvinylidene fluoride membranes. Following blocking with 5% nonfat dried milk in Tris-buffered saline containing 0.05% Tween 20 at room temperature for 1 h, the membranes were incubated with primary antibodies against α-ENaC (1:300; sc-21012), β-ENaC (1:300; sc-21013), γ-ENaC (1:300; sc-21014), PI3K p85α (1:1,000; sc-71892), SGK1 (1:500; sc-33774), phosphorylated-SGK1 (Ser422; 1:500; sc-16745) all from Santa Cruz Biotechnology, Inc. and β-actin (1:500, bsm-33036M, BIOSS, Beijing, China) overnight at 4˚C, and then incubated
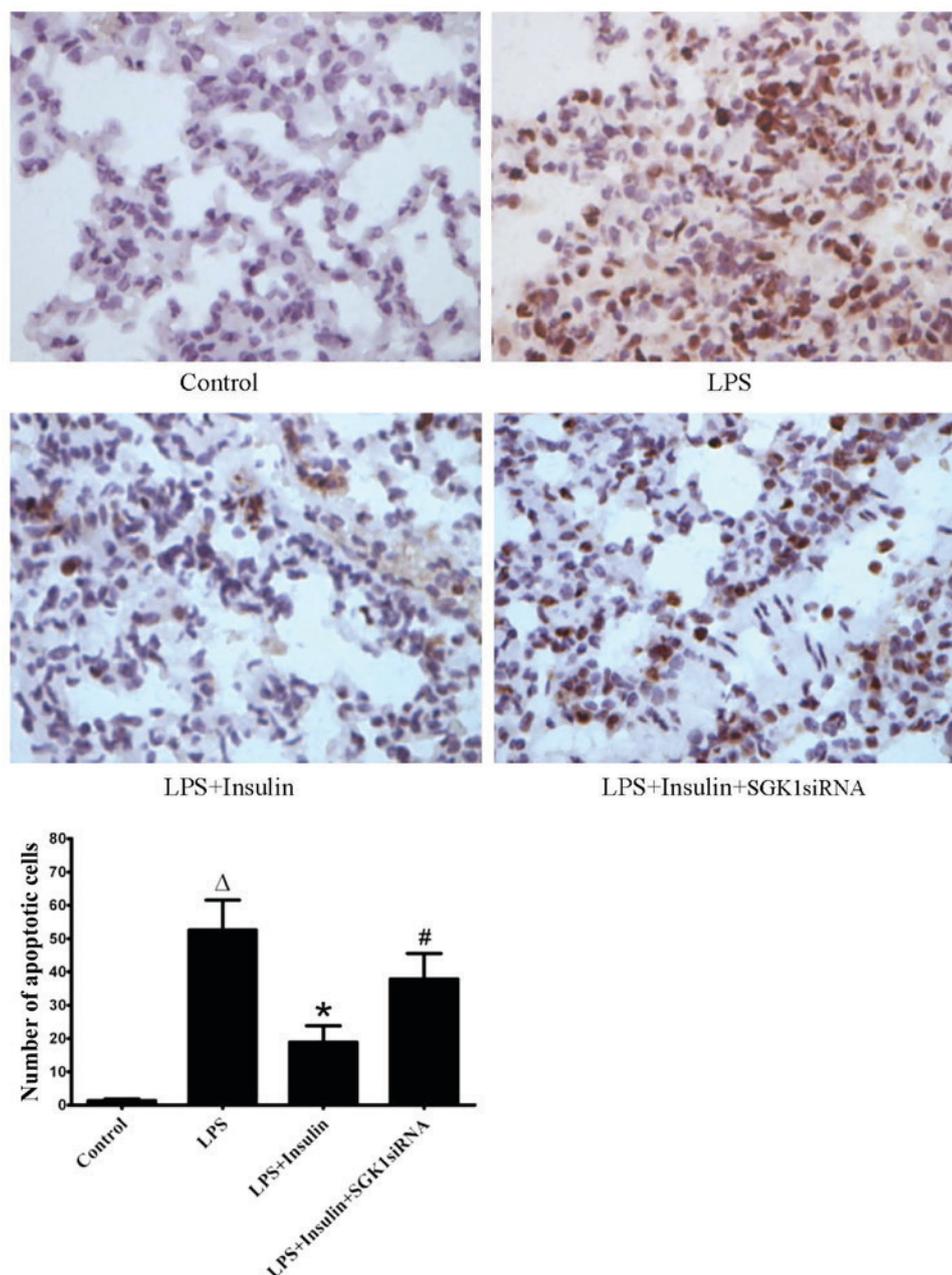
Figure 5. Effect of exogenous insulin on apoptosis in mice with LPS-induced lung injury (n=6 per group). The numbers of apoptotic alveolar epithelial cells (brown-stained) were counted in five randomly selected high-power fields for each section (magnification, x400), and the mean value was calculated. Data are presented as the mean ± standard error. $^{\Delta}$P<0.01 vs. control group; *P<0.01 vs. LPS group; $^{\#}$P<0.05 vs. LPS + insulin group. LPS, lipopolysaccharide; SGK1, serum/glucocorticoid-inducible kinase-1; siRNA, small interfering RNA.

with horseradish peroxidase-conjugated secondary antibody (1:5,000) at room temperature for 1.5 h. Using enhanced chemiluminescence (KeyGen Biotech Co., Ltd.), the protein bands were visualized by a UVP gel imaging system (Analytik Jena, Upland, CA, USA) and analyzed by Labworks software (version 4.6; Labworks LLC, Lehi, UT, USA).

Statistical analysis. All data are presented as the mean ± standard error of the mean. Student's t-test and one-way analysis of variance were performed. SPSS version 12.0 software (SPSS, Inc., Chicago, IL, USA) was used for the statistical analysis. P<0.05 was considered to indicate a statistically significant difference.

Results

The effect of siRNA transfection in mouse lung tissues and primary alveolar epithelial cells. As observed in Fig. 1A, transfection with SGK1 siRNA resulted in evident downregulation of SGK1 expression in mouse lung tissues, as compared with the control and scramble siRNA groups. As shown in Fig. 1B, PI3K siRNA and SGK1 siRNA also significantly decreased PI3K and SGK1 protein expression levels in primary alveolar epithelial cells, respectively.

Effect of exogenous insulin on plasma glucose levels. No significant differences were observed in the plasma glucose
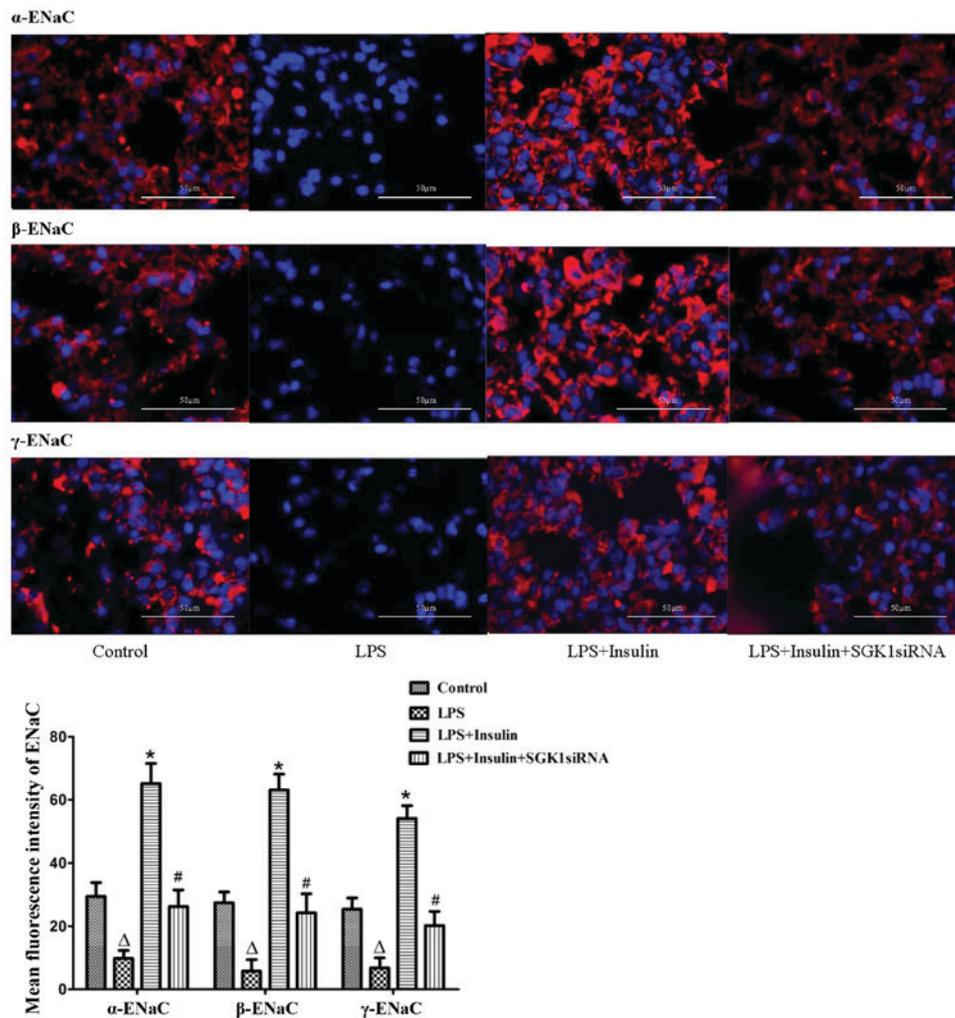
Figure 6. Effect of exogenous insulin on the location and expression of α-, β- and γ-ENaC in the lungs of mice at 24 h after LPS-induced lung injury was examined by laser scanning confocal microscopy, and the fluorescence intensities were determined (n=6 per group). Scale bar, 50 μM. Nuclear DNA was counterstained with DAPI (blue). Data are presented as the mean ± standard error. $^{\Delta}$P<0.05 vs. control group; *P<0.01 vs. LPS group; $^{#}$P<0.05 vs. LPS + insulin group. LPS, lipopolysaccharide; SGK1, serum/glucocorticoid-inducible kinase-1; siRNA, small interfering RNA.

levels of normal mice treated with insulin for 0, 30, 60, 120 and 240 min (Table I). In addition, no significant differences were observed in the plasma glucose levels of insulin- and saline-treated mice at 0, 1, 4 and 8 h in the LPS-induced lung injury group. The results indicated that insulin did not alter the glucose level during ALI (Table II).

Exogenous insulin protects the pulmonary epithelial barrier in LPS-induced lung injury. Insulin treatment significantly decreased the LPS-induced increase in total protein, total cell numbers and neutrophils in BALF (Fig. 2A-C). However, the delivery of SGK1 siRNA significantly blocked the effect of insulin in the LPS-induced lung injury group (Fig. 2A-C). The pulmonary epithelial barrier was injured in mice with LPS-induced lung injury, as indicated by the increase in the BALF/serum fluorescence ratio, which was a result of high bronchoalveolar epithelial permeability (Fig. 2D). The BALF/serum fluorescence ratio was significantly decreased by insulin, indicating a decreased bronchoalveolar epithelial permeability; thus, insulin exerted a protective effect on pulmonary epithelial barrier function in ALI. However, SGK1 siRNA clearly blocked the effect of insulin, as

evidenced by the marked increase in the BALF/serum fluorescence ratio (Fig. 2D).

Exogenous insulin attenuates LPS-induced lung injury. The pulmonary morphology of ALI mice demonstrated significant injury, with the presence of severe interstitial edema, thickened alveolar septa, inflammatory cell infiltration and formation of proteinaceous debris in the alveolar spaces, as compared with the control mice (Fig. 3A and B). Insulin treatment significantly attenuated the LPS-induced lung injury (Fig. 3C), while the lung injury was significantly aggravated with the co-administration of SGK1 siRNA (Fig. 3D). The lung injury score supported the observation that insulin ameliorated LPS-induced lung injury and that SGK1 siRNA blocked the effect of insulin in ALI mice (Fig. 3E).

Exogenous insulin attenuates pulmonary edema and improves AFC in LPS-induced lung injury. Insulin induced a decrease in the wet-to-dry ratio and increase in AFC in mice with LPS-induced lung injury at 6, 12 and 24 h (Fig. 4A and B). In addition, exposure to amiloride, a sodium channel inhibitor, inhibited the insulin-induced AFC in mice with LPS-induced
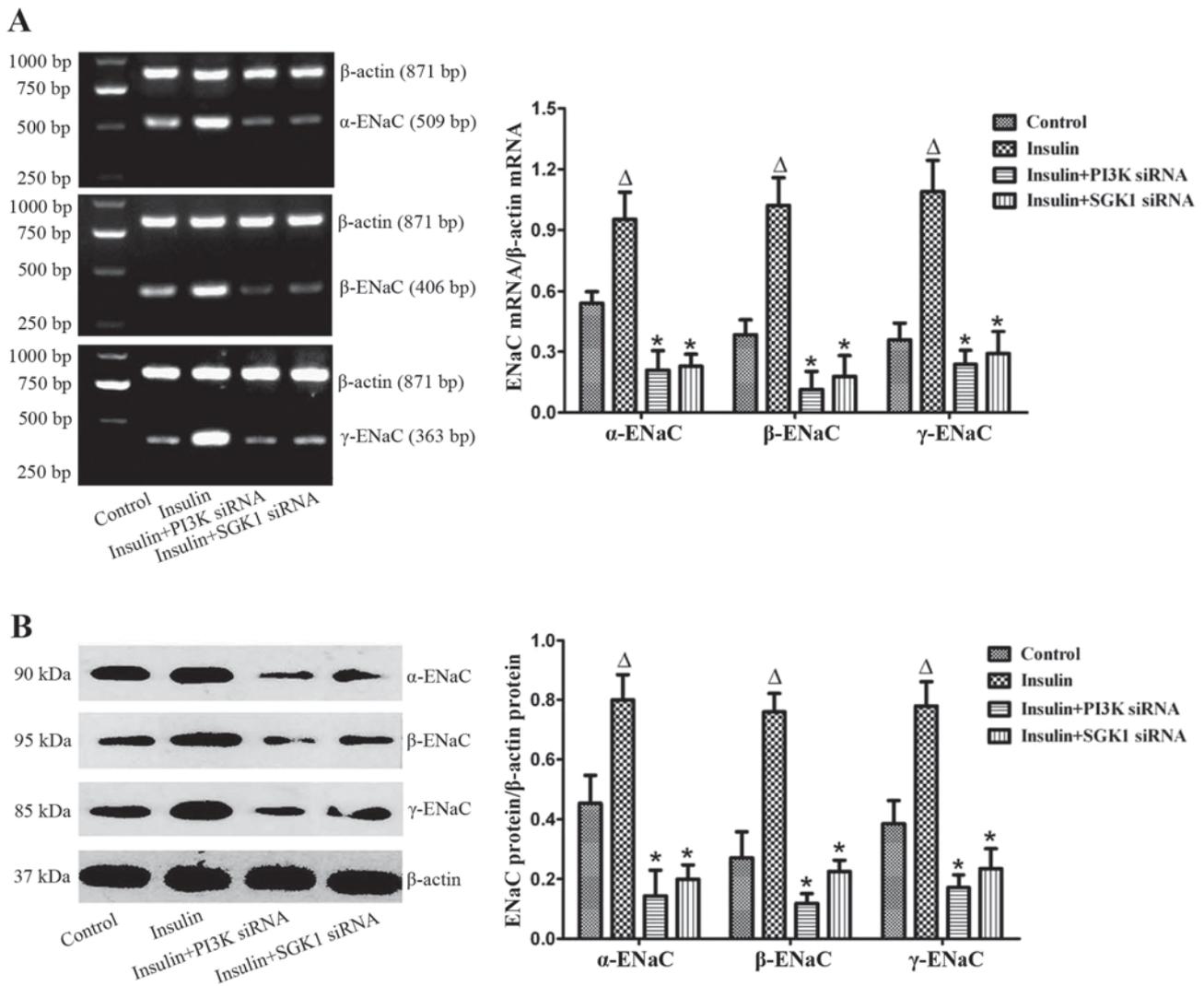
Figure 7. Effect of exogenous insulin on the expression levels of α-, β- and γ-ENaC in alveolar epithelial cells following transfection with control siRNA, PI3K siRNA or SGK1 siRNA, examined by (A) RT-PCR and (B) western blotting. At 72 h after transfection, primary alveolar epithelial cells were incubated with or without 200 mU/l insulin for 2 h, and then RT-PCR and western blotting were performed. The band intensity of α-, β- and γ-ENaC was quantified by normalizing it to β-actin. Data are presented as the mean ± standard error. $^{\Delta}$P<0.01 vs. control group; *P<0.01 vs. insulin group. ENaC, epithelial sodium channel; PI3K, phosphatidylinositol 3-kinase; SGK1, serum/glucocorticoid-inducible kinase-1; siRNA, small interfering RNA; RT-PCR, reverse transcription polymerase chain reaction.

lung injury (Fig. 4B). It was also observed that SGK1 siRNA significantly blocked the insulin-induced decrease in the wet-to-dry ratio (Fig. 4C). Furthermore, insulin significantly increased AFC (by 93%) in the LPS-induced lung injury group; however, this effect was significantly inhibited by treatment with amiloride or SGK1 siRNA, which resulted in a 60 and 33% decrease in AFC, respectively, as compared with the LPS + insulin group (Fig. 4D).

Effect of exogenous insulin on apoptosis in LPS-induced lung injury. The total number of apoptotic cells in the LPS-induced lung injury group was significantly higher as compared with that in the control group. Treatment with insulin reduced the number of apoptotic cells in the ALI group. However, SGK1 siRNA reversed the effect of insulin on the apoptosis of alveolar epithelial cells (Fig. 5).

Exogenous insulin increases the expression of ENaC in vivo and in vitro. α-, β- and γ-ENaC expression was examined by

immunofluorescence in the LPS-induced lung injury group (Fig. 6). In normal mice, α-, β- and γ-ENaC were localized in the alveolar epithelium. However, the distribution and expression of α-, β- and γ-ENaC were clearly reduced in the LPS-induced lung injury group. Immunostaining of α-, β- and γ-ENaC were significantly increased by insulin treatment, while the insulin-induced expression of α-, β- and γ-ENaC was clearly blocked by SGK1 siRNA (Fig. 6). Furthermore, in the primary alveolar epithelial cells, insulin significantly increased the mRNA and protein expression levels of α-, β- and γ-ENaC; however, this insulin-induced effect was inhibited in cells transfected with PI3K siRNA or SGK1 siRNA (Fig. 7). These results indicated that insulin improved AFC by upregulating ENaC expression via the PI3K/SGK1 pathway.

Exogenous insulin activates the PI3K/SGK1 pathway in vivo and in vitro. The level of phosphorylated SGK1 was markedly increased by insulin in the LPS-induced lung injury group; however, SGK1 siRNA reversed the insulin-induced increase
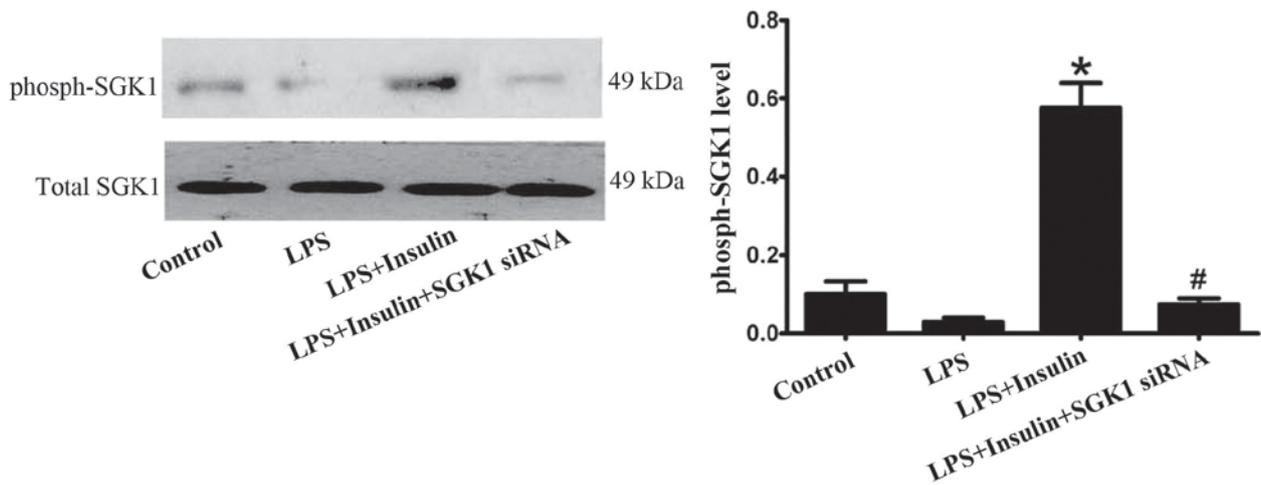
Figure 8. Effect of exogenous insulin on the expression of phosphorylated SGK1 in the lungs of mice at 24 h after LPS-induced lung injury (n=3 per group). The band intensity of phosphorylated SGK1 was quantified by normalizing it to total SGK1 and is expressed as the fold of the control. Data are presented as the mean ± standard error. [*]P<0.01 vs. LPS group; [#]P<0.01 vs. LPS + insulin group. LPS, lipopolysaccharide; SGK1, serum/glucocorticoid-inducible kinase-1; siRNA, small interfering RNA.
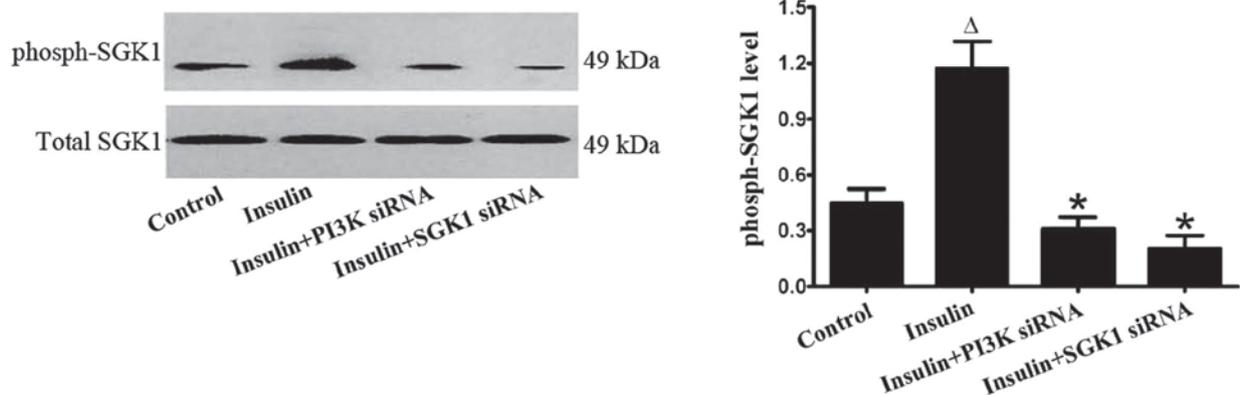
Figure 9. Effect of exogenous insulin on the expression of phosphorylated SGK1 in primary alveolar epithelial cells following transfection with control, PI3K or SGK1 siRNAs. At 72 h after transfection, primary alveolar epithelial cells were incubated with or without 200 mU/l insulin for 2 h, and then western blotting was performed. The band intensity of phosphorylated SGK1 was quantified by normalizing it to total SGK1 and is expressed as the fold of the control. Data are presented as the mean ± standard error. [Δ]P<0.05 vs. control group; [*]P<0.01 vs. insulin group. PI3K, phosphatidylinositol 3-kinase; SGK1, serum/glucocorticoid-inducible kinase-1; siRNA, small interfering RNA.

in the level of phosphorylated SGK1 (Fig. 8). In primary alveolar epithelial cells, insulin significantly increased the level of phosphorylated SGK1; however, the effect of insulin was markedly inhibited by the transfection with PI3K siRNA or SGK1 siRNA (Fig. 9). These findings strongly indicated that insulin regulated the ENaC expression via the PI3K/SGK1 pathway in LPS-induced lung injury.

Discussion

The present study results demonstrated that insulin protected the lung epithelium and attenuated pulmonary edema by improving AFC through the upregulation of ENaC via the PI3K/SGK1 pathway in LPS-induced lung injury. A model of ALI without hyperglycemia was used to maintain the glucose levels within the normal range since hyperglycemia contributes to the inflammatory response, and lung injury is attenuated by insulin treatment in euglycemia (24-26). Previous results from clinical studies have confirmed that

glucose control is very important in critically ill patients, leading to decreased mortality and morbidity (27,28). In addition, the dose and rate of human insulin infused by micro-osmotic pumps in the present study had an anti-inflammatory effect rather than an effect on the modulation of glucose metabolism, since it was observed that insulin treatment did not affect the glucose levels in the LPS-induced lung injury group.

Toll-like receptor 4 (TLR4) is detected in a number of immune cells, including monocytes, macrophages, dendritic cells and several T cell populations, and is part of the receptor complex that binds LPS from the Gram-negative bacterial cell wall and endogenous ligands, including heat-shock proteins and other inflammatory mediators (29). LPS-induced activation of TLR4 leads to the dimerization of TLR4 monomers and the generation of nucleus-seeking nuclear factor (NF)-κB transcription factors. Numerous pro-inflammatory cytokine and chemokine genes contain NF-κB response elements in their promoter regions, such as tumor necrosis factor-α and

interleukin-6 (30). LPS-stimulated cytokine release is achieved through the TLR4-mediated NF-κB signaling pathway (31).

Different inflammatory mediators, such as cytokines, are released following LPS stimulation to recruit activated neutrophils into the injured lung, which is the main cause of pulmonary edema and the development of ALI (32,33). Activated neutrophils migrate into alveolar spaces and pulmonary epithelium by CXC chemokines, which lead to alveolar capillary barrier leakage, and interstitial and alveolar edema by reactive oxygen species (33,34). In the present study, LPS was administered to establish a well-characterized model of ALI, resulting in an increase in protein, total cell count and neutrophils in the BALF, as well as an elevation in bronchoalveolar epithelial permeability, which indicated alveolar capillary barrier damage. Increased alveolar capillary permeability results in edema fluid accumulation in the alveolar spaces. Treatment with insulin protected the alveolar capillary barrier that was damaged as a result of the LPS-induced lung injury; however, SGK1 siRNA reversed the protective effect of insulin. In addition, LPS-treated mice exhibited typical pathological alterations, such as interstitial edema, thickened alveolar septa, proteinaceous debris and inflammatory cell infiltration in the alveolar space. Insulin treatment alleviated these pathological changes, whereas this alleviation was inhibited by SGK1 siRNA. The results indicated that insulin attenuated pulmonary edema with the involvement of SGK1.

It is well recognized that AFC is an effective way to remove edema from the alveolar spaces (35). In the present study, insulin improved AFC and decreased pulmonary edema in the LPS-induced lung injury group. However, SGK1 siRNA blocked the effect of insulin on AFC in the LPS-treated group, which indicated the essential involvement of SGK1. In addition, the use of amiloride, a sodium channel inhibitor, inhibited the insulin-stimulated AFC. This supported the result that ENaC may participate in AFC, which is consistent with the findings of previous studies (24,36).

Lung epithelium injury was also reported to be a determinant for the development of protein-rich pulmonary edema in ARDS (37). In particular, lung epithelial apoptosis is considered to be an important pathogenetic mechanism in ALI (38,39). An acceleration of lung epithelial cell apoptosis may contribute to the destruction of the alveolar epithelial barrier, a promotion of protein-rich edema in the alveoli and altered fluid clearance from the alveolar space in ALI/ARDS (1,40). In the present study, insulin exerted a protective effect on the lung epithelium by reducing the apoptosis of alveolar epithelial cells, indicating the alleviation of pulmonary edema and the important role of SGK1 in the protection against cell apoptosis, as described previously (41).

We previously reported that ENaC served an important role in the regulation of sodium and water balance in AFC (24,42,43). Therefore, the regulation of ENaC by insulin, possibly via the PI3K/SGK1 signaling pathway, was further investigated in the current study. SGK1, a serine/threonine protein kinase, was reported to be a key regulator of sodium transport by hormones, such as insulin, in mammalian epithelia (44-47). Furthermore, the activation of SGK1 was dependent on the phosphorylation of S422 in the hydrophobic motif at its COOH terminus by the PI3K-dependent pyruvate dehydrogenase kinase 2 pathway (47,48). It has been recognized that a central function of

activated SGK1 was to increase the expression of ENaC in the cell surface by inhibiting the ubiquitin ligase Nedd4-2 (49,50). In the present study, the expression levels of α-, β- and γ-ENaC, and the level of phosphorylated SGK1 were increased by insulin treatment, whereas these were decreased by co-treatment with SGK1 siRNA in the LPS-induced lung injury group. *In vitro*, PI3K siRNA or SGK1 siRNA prevented the insulin-induced increase in the expression levels of α-, β- and γ-ENaC, and phosphorylated SGK1. The increased expression of ENaC by insulin-induced SGK1 was possibly dependent on the phosphorylation of Nedd4-2 in a PY motif-dependent manner (50,51). Taken together, in the present study, the effect of insulin on AFC was further illustrated through the upregulation of α-, β- and γ-ENaC via the PI3K/SGK1 signaling pathway, which was a further investigation of our previous findings (18).

In conclusion, the present results demonstrated that insulin protected the lung epithelium and attenuated pulmonary edema in mice with LPS-induced lung injury, without affecting the blood glucose levels, and this effect was achieved through the upregulation of ENaC via the PI3K/SGK1 pathway. While further research is required to fully understand the role of insulin in the complex mechanisms of ALI/ARDS, the present study provides novel evidence of the protective role of insulin in AFC associated with ALI.

Availability of data and material

All data analyzed during the present study are included in the published article. The raw datasets used for the analysis are available from the corresponding author on reasonable request.

Authors' contributions

WD and DW participated in the design of the study. CL and JT performed the animal experiments. JH and YZ performed the immunocytochemistry, RT-qPCR and western blotting assays. WD and DW performed the statistical analysis, interpreted the data and drafted the manuscript. WD and DW are accountable for all aspects of the work. All authors contributed to the interpretation of the data and critical revision of the manuscript. Each individual author read and approved the final manuscript.

Ethics approval and consent to participate

All animal experiments were approved by the Ethics Committee of the Second Affiliated Hospital of Chongqing Medical University (Chongqing, China).

Patient consent for publication

Not applicable.

Competing interests

The authors declare that they have no competing interests.

References

1. Máca J, Jor O, Holub M, Sklienka P, Burša F, Burda M, Janout V and Ševčík P: Past and present ARDS mortality rates: A systematic review. Respir Care 62: 113-122, 2017.
2. Villar J, Sulemanji D and Kacmarek RM: The acute respiratory distress syndrome: Incidence and mortality, has it changed? Curr Opin Crit Care 20: 3-9, 2014.
3. Azzam ZS and Sznajder JI: Lung edema clearance: Relevance to patients with lung injury. Rambam Maimonides Med J 6, 2015.
4. Berthiaume Y and Matthay MA: Alveolar edema fluid clearance and acute lung injury. Respir Physiol Neurobiol 159: 350-359, 2007.
5. Matalon S, Bartoszewski R and Collawn JF: Role of epithelial sodium channels in the regulation of lung fluid homeostasis. Am J Physiol Lung Cell Mol Physiol 309: L1229-L1238, 2015.
6. Lee JW, Krasnodembskaya A, McKenna DH, Song Y, Abbott J and Matthay MA: Therapeutic effects of human mesenchymal stem cells in ex vivo human lungs injured with live bacteria. Am J Respir Crit Care Med 187: 751-760, 2013.
7. Folkesson HG and Matthay MA: Alveolar epithelial ion and fluid transport: Recent progress. Am J Respir Cell Mol Biol 35: 10-19, 2006.
8. Hummler E, Barker P, Gatzy J, Beermann F, Verdumo C, Schmidt A, Boucher R and Rossier BC: Early death due to defective neonatal lung liquid clearance in alpha-ENaC-deficient mice. Nat Genet 12: 325-328, 1996.
9. Randrianarison N, Clerici C, Ferreira C, Fontayne A, Pradervand S, Fowler-Jaeger N, Hummler E, Rossier BC and Planès C: Low expression of the beta-ENaC subunit impairs lung fluid clearance in the mouse. Am J Physiol Lung Cell Mol Physiol 294: L409-L416, 2008.
10. Elias N, Rafii B, Rahman M, Otulakowski G, Cutz E and O'Brodovich H: The role of alpha-, beta-, and gamma-ENaC subunits in distal lung epithelial fluid absorption induced by pulmonary edema fluid. Am J Physiol Lung Cell Mol Physiol 293: L537-L545, 2007.
11. Marone R, Cmiljanovic V, Giese B and Wymann MP: Targeting phosphoinositide 3-kinase: Moving towards therapy. Biochim Biophys Acta 1784: 159-185, 2008.
12. Record RD, Froelich LL, Vlahos CJ and Blazer-Yost BL: Phosphatidylinositol 3-kinase activation is required for insulin-stimulated sodium transport in A6 cells. Am J Physiol 274: E611-E617, 1998.
13. Blazer-Yost BL, Esterman MA and Vlahos CJ: Insulin-stimulated trafficking of ENaC in renal cells requires PI3-kinase activity. Am J Physiol Cell Physiol 284: C1645-C1653, 2003.
14. Cohen P: The origins of protein phosphorylation. Nat Cell Biol 4: E127-E130, 2002.
15. Soundararajan R, Melters D, Shih IC, Wang J and Pearce D: Epithelial sodium channel regulated by differential composition of a signaling complex. Proc Natl Acad Sci USA 106: 7804-7809, 2009.
16. Perrotti N, He RA, Phillips SA, Haft CR and Taylor SI: Activation of serum- and glucocorticoid-induced protein kinase (Sgk) by cyclic AMP and insulin. J Biol Chem 276: 9406-9412, 2001.
17. Liu ML, Dong HY, Zhang B, Zheng WS, Zhao PT, Liu Y, Niu W, Xu DQ and Li ZC: Insulin reduces LPS-induced lethality and lung injury in rats. Pulm Pharmacol Ther 25: 472-477, 2012.
18. Zhu T, Zhang W and Wang DX: Insulin up-regulates epithelial sodium channel in LPS-induced acute lung injury model in rats by SGK1 activation. Injury 43: 1277-1283, 2012.
19. Zhang X, Huang H, Yang T, Ye Y, Shan J, Yin Z and Luo L: Chlorogenic acid protects mice against lipopolysaccharide-induced acute lung injury. Injury 41: 746-752, 2010.
20. Dobbs LG: Isolation and culture of alveolar type II cells. Am J Physiol 258: L134-L147, 1990.
21. Lomas-Neira JL, Chung CS, Wesche DE, Perl M and Ayala A: In vivo gene silencing (with siRNA) of pulmonary expression of MIP-2 versus KC results in divergent effects on hemorrhage-induced, neutrophil-mediated septic acute lung injury. J Leukoc Biol 77: 846-853, 2005.

22. Matute-Bello G, Downey G, Moore BB, Groshong SD, Matthay MA, Slutsky AS and Kuebler WM; Acute Lung Injury in Animals Study Group: An official American Thoracic Society workshop report: Features and measurements of experimental acute lung injury in animals. Am J Respir Cell Mol Biol 44: 725-738, 2011.
23. Sakuma T, Hida M, Nambu Y, Osanai K, Toga H, Takahashi K, Ohya N, Inoue M and Watanabe Y: Effects of hypoxia on alveolar fluid transport capacity in rat lungs. J Appl Physiol (1985) 91: 1766-1774, 2001.
24. Deng W, Li CY, Tong J, Zhang W and Wang DX: Regulation of ENaC-mediated alveolar fluid clearance by insulin via PI3K/Akt pathway in LPS-induced acute lung injury. Respir Res 13: 29, 2012.
25. Hagiwara S, Iwasaka H, Hasegawa A, Koga H and Noguchi T: Effects of hyperglycemia and insulin therapy on high mobility group box 1 in endotoxin-induced acute lung injury in a rat model. Crit Care Med 36: 2407-2413, 2008.
26. Chen HI, Yeh DY, Liou HL and Kao SJ: Insulin attenuates endotoxin-induced acute lung injury in conscious rats. Crit Care Med 34: 758-764, 2006.
27. Fahy BG, Sheehy AM and Coursin DB: Glucose control in the intensive care unit. Crit Care Med 37: 1769-1776, 2009.
28. van den Berghe G, Wouters P, Weekers F, Verwaest C, Bruyninckx F, Schetz M, Vlasselaers D, Ferdinande P, Lauwers P and Bouillon R: Intensive insulin therapy in critically ill patients. N Engl J Med 345: 1359-1367, 2001.
29. Stevens CW, Aravind S, Das S and Davis RL: Pharmacological characterization of LPS and opioid interactions at the toll-like receptor 4. Br J Pharmacol 168: 1421-1429, 2013.
30. Kenny EF and O'Neill LA: Signaling adaptors used by Toll-like receptors: An update. Cytokine 43: 342-349, 2008.
31. Guijarro-Muñoz I, Compte M, Álvarez-Cienfuegos A, Álvarez-Vallina L and Sanz L: Lipopolysaccharide activates Toll-like receptor 4 (TLR4)-mediated NF-κB signaling pathway and proinflammatory response in human pericytes. J Biol Chem 289: 2457-2468, 2014.
32. Abraham E: Neutrophils and acute lung injury. Crit Care Med 31: S195-S199, 2003.
33. Reutershan J and Ley K: Bench-to-bedside review: Acute respiratory distress syndrome-how neutrophils migrate into the lung. Crit Care 8: 453-461, 2004.
34. Fialkow L, Wang Y and Downey GP: Reactive oxygen and nitrogen species as signaling molecules regulating neutrophil function. Free Radic Biol Med 42: 153-164, 2007.
35. Eaton DC, Helms MN, Koval M, Bao HF and Jain L: The contribution of epithelial sodium channels to alveolar function in health and disease. Annu Rev Physiol 71: 403-423, 2009.
36. Bellmeyer A, Martino JM, Chandel NS, Scott Budinger GR, Dean DA and Mutlu GM: Leptin resistance protects mice from hyperoxia-induced acute lung injury. Am J Respir Crit Care Med 175: 587-594, 2007.
37. Matthay MA and Zemans RL: The acute respiratory distress syndrome: Pathogenesis and treatment. Annu Rev Pathol 6: 147-163, 2011.
38. Martin TR, Nakamura M and Matute-Bello G: The role of apoptosis in acute lung injury. Crit Care Med 31: S184-S188, 2003.
39. Perl M, Lomas-Neira J, Chung CS and Ayala A: Epithelial cell apoptosis and neutrophil recruitment in acute lung injury-a unifying hypothesis? What we have learned from small interfering RNAs. Mol Med 14: 465-475, 2008.
40. Gropper MA and Wiener-Kronish J: The epithelium in acute lung injury/acute respiratory distress syndrome. Curr Opin Crit Care 14: 11-15, 2008.
41. Mikosz CA, Brickley DR, Sharkey MS, Moran TW and Conzen SD: Glucocorticoid receptor-mediated protection from apoptosis is associated with induction of the serine/threonine survival kinase gene, sgk-1. J Biol Chem 276: 16649-16654, 2001.
42. Deng J, Wang DX, Deng W, Li CY, Tong J and Ma H: Regulation of alveolar fluid clearance and ENaC expression in lung by exogenous angiotensin II. Respir Physiol Neurobiol 181: 53-61, 2012.
43. Deng W, Wang DX, Zhang W and Li CY: Regulation of epithelial sodium channel α-subunit expression by adenosine receptor A$_2$a in alveolar epithelial cells. Chin Med J (Engl) 124: 1551-1555, 2011.
44. Lang F, Bohmer C, Palmada M, Seebohm G, Strutz-Seebohm N and Vallon V: (Patho)physiological significance of the serum- and glucocorticoid-inducible kinase isoforms. Physiol Rev 86: 1151-1178, 2006.

45. Loffing J, Flores SY and Staub O: Sgk kinases and their role in epithelial transport. Annu Rev Physiol 68: 461-490, 2006.

46. Wulff P, Vallon V, Huang DY, Völkl H, Yu F, Richter K, Jansen M, Schlünz M, Klingel K, Loffing J, et al: Impaired renal Na(+) retention in the sgk1-knockout mouse. J Clin Invest 110: 1263-1268, 2002.

47. Webster MK, Goya L, Ge Y, Maiyar AC and Firestone GL: Characterization of sgk, a novel member of the serine/threonine protein kinase gene family which is transcriptionally induced by glucocorticoids and serum. Mol Cell Biol 13: 2031-2040, 1993.

48. Park J, Leong ML, Buse P, Maiyar AC, Firestone GL and Hemmings BA: Serum and glucocorticoid-inducible kinase (SGK) is a target of the PI3-kinase-stimulated signaling pathway. EMBO J 18: 3024-3033, 1999.

49. Snyder PM, Olson DR and Thomas BC: Serum and glucocorticoid-regulated kinase modulates Nedd4-2-mediated inhibition of the epithelial Na+ channel. J Biol Chem 277: 5-8, 2002.

50. Debonneville C, Flores SY, Kamynina E, Plant PJ, Tauxe C, Thomas MA, Münster C, Chraïbi A, Pratt JH, Horisberger JD, et al: Phosphorylation of Nedd4-2 by Sgk1 regulates epithelial Na(+) channel cell surface expression. EMBO J 20: 7052-7059, 2001.

51. Wiemuth D, Lott JS, Ly K, Ke Y, Teesdale-Spittle P, Snyder PM and McDonald FJ: Interaction of serum- and glucocorticoid regulated kinase 1 (SGK1) with the WW-domains of Nedd4-2 is required for epithelial sodium channel regulation. PLoS One 5: e12163, 2010.